Electronic Supplementary Information for

Control over preference for binding sites of polyoxometalates to silver ethynide clusters by surface charge modification

Sho Tamari,[a] Kosuke Ono,[b] Masato Hashimoto[c] and Tomoji Ozeki[d,]*

[a] Department of Chemistry and Materials Science, Tokyo Institute of Technology, 2-12-1 O-okayama, Meguro-ku, Tokyo 152-8551, Japan.
[b] Department of Chemistry, Faculty of Science, Tokyo University of Science, 1-3 Kagurazaka, Shinjuku-ku, Tokyo 162-8601, Japan.
[c] Department of Material Science and Chemistry, Faculty of Systems Engineering, Wakayama University, 930 Sakaedani, Wakayama 640-8510, Japan.
[d] Department of Chemistry, College of Humanities and Sciences, Nihon University, 3-25-40 Sakurajosui, Setagaya-ku, Tokyo 156-8550, Japan.

*To whom the correspondence should be addressed. E-mail: ozeki@chs.nihon-u.ac.jp.

Contents

Experimental details

Reagents and general procedure

The following were purchased from commercial sources and used without further purification: 99 % CF_3SO_3Ag (Aldrich), 99.8 % $AgNO_3$ (Kokusan Kagaku), 96 % 3,3-dimethyl-1-butyne (^{t}BuC≡CH, TCI), 85 % KOH (Koso), 98 % (n-C_4H_9)$_4$NBr (Tokyo Kasei), 99 % $Na_2WO_4 \cdot 2H_2O$, 99.9 % Nb_2O_5, 99.5 % NaCl, 98 % $Na_2SiO_3 \cdot 9H_4O$, 64.0–67.4 % $NaHSO_3$, 30–35 % H_2O_2, 35–37 % hydrochloric acid, 28–30 % ammonia water, 10 % (n-C_4H_9)$_4$NOH aqueous solution, 99.8 % CH_3OH, 99.5 % C_2H_5OH, 99.5 % diethylether (Wako), 99.5 % CH_3CN (Nacalai Tesque).

Elemental analyses for C, H, Ag, N, Nb, O, Si and W were performed by Mikroanalytisches Labor Pascher (Remagen-Bandorf, Germany). Infrared absorption spectrum was recorded as a KBr pellet on a JASCO FT/IR-460 Plus spectrometer.

Single crystal X-ray diffraction

A colorless crystal with the dimension of 0.15 × 0.15 × 0.05 mm was mounted in a nitrogen stream at 123 K immediately picking up from the mother liquor onto a Rigaku Mercury CCD diffractometer controlled by CrystalClear[1] on the KEK-PF AR-NW2A synchrotron beamline (λ = 0.6890 Å). Diffraction images were indexed, integrated and scaled by HKL2000.[2] The integrated data were corrected for absorption using PLATON MULABS.[3] The structure was determined by the charge flipping method using SUPERFLIP[4] and refined by the full-matrix least-squares method on F^2 using the SHELXL-2014[5] with the aid of WinGX program package.[6] Anisotropic displacement parameters were applied to all the non-hydrogen atoms. Hydrogen atoms of the *tert*-butyl groups were included using the riding model and those of the acetonitrile molecules were not determined.

During the refinement, type C Ag atoms (Ag19–Ag24; see Table S1 for the correspondence between the type codes and the atom numbering) showed large atomic displacement parameters (ADPs) and relatively high residual electron density maxima were observed at their proximities. We interpreted that type C Ag atoms are disordered over originally located sites (Ag19–Ag24) and these electron density maxima (labeled as Ax19–Ax24). As listed in Table S2, each of Ag19–Ag24 is bonded to three C(terminal *sp*) atoms [two from type b C≡C^{t}Bu, 2.34(2)–2.52(3) Å, average 2.45 Å and one from type d C≡C^{t}Bu, 2.136(19)–2.20(2) Å, average 2.18 Å] while each of Ax19–Ax24 is bonded to only one C(terminal *sp*) atom [from type d C≡C^{t}Bu, 2.13(2)–2.19(3) Å, average 2.16 Å]. Instead, each of Ax19–Ax24 is bonded to a μ_2-O(corner sharing Nb_2) [2.14(3)–2.211(13) Å, average 2.17 Å], a μ_2-O(edge sharing NbW) [2.72(3)–2.912(19) Å, average 2.82 Å] and a μ_2-O(corner sharing W_2) [3.01(6)–3.22(4) Å, average 3.13 Å], while Ag19–Ag24 have no short contact to the polyoxometalate O atoms.

The C≡C^{t}Bu ligands in the proximity of Ag19–Ag24 and Ax19–Ax24 (types b and d) do not exhibit apparent effect by this disorder. It is probably because all the C≡C^{t}Bu ligands are closely packed into a congested environment (see Figure 2) and the terminal C atoms of the C≡C^{t}Bu ligands firmly bind to the Ag_{42} core. The terminal C atom of a type b ligand has one bond (2.089–2.141 Å) to type A Ag atom, two bonds (2.47–2.70 Å) to type B Ag atoms, and two bonds (2.34–2.52 Å) to type C Ag atoms. Dislocation of a Ag atom from type C site to type X site results in a loss of a very weak bond to type C Ag atom (2.34–2.52 Å), but its influence may be limited. The terminal C atom of a type d ligand has one bond (2.136–2.20 Å) to type C Ag atom and two bonds (2.16–2.29 Å) to type E Ag atoms. Dislocation of a Ag atom from type C site to type X site results in a loss of one bond to type C Ag atom (2.136–2.20 Å), which may be compensated by the formation of one bond to type X Ag atom (2.13–2.19 Å).

Sum of the site occupancies for each pair (Ag*n* and Ax*n*, where n = 19–24) were constrained to be 1.0. The occupancies for these six Ax sites (See Table S2) sum to 1.022, which means that one of the six type C Ag atoms occupies the Ax site in one molecule.

The calculation of solvent accessible void by Mercury 3.6[7] with the probe radius of 1.2 Å and grid spacing of 0.1 Å indicated that 21.0 % (3398.4 $Å^3$) of the unit cell remain unoccupied and could be filled by solvents or guest molecules. During the refinement, the void was not modelled either by individual molecules or by continuous electron density.

The structural illustrations were prepared by using Diamond 3.2k.[8] Crystallographic data have been deposited with Cambridge Crystallographic Data Centre with the Deposition number of CCDC-1413590. Copies of the data can be obtained free of charge via www.ccdc.cam.ac.uk/data_request/cif (or from the Cambridge Crystallographic Data Centre, 12, Union Road, Cambridge, CB2 1EZ, U.K.; Fax: +44 1223 336033; e-mail: deposit@ccdc.cam.ac.uk).

Powder X-ray diffraction

Powder X-ray diffraction pattern was measured at room temperature in a transmission geometry on a Rigaku Smart Lab diffractometer using CuKα radiation (λ = 1.54184 Å). Samples were ground in and sealed with the mother liquor. The whole observed diffraction pattern was fitted by the Pawley method using Topas 5.0.[9] Refined lattice constants are listed in Table S4 together with those obtained from the single crystal diffraction at 123 K. Observed pattern was also compared with the simulated pattern calculated by Mercury 3.5.1[7] using the crystal and atomic data obtained from the single crystal X-ray diffraction at 123 K.

The Pawley refinement gave a satisfactory fitting (see Figure S8) with lattice constants slightly different from that obtained from the single crystal diffraction (see Table S4), which is reasonably attributed to the temperature difference (powder diffraction at room temperature and single crystal diffraction at 123 K). Simulated pattern based of the result of single crystal diffraction also matches well with the observed pattern except for the systematic deviation of peak positions due to the contraction of the crystal lattice at low temperature.

NMR

^{1}H, ^{13}C and NOESY NMR spectra were recorded on a Bruker DRX-500 (500 MHz for ^{1}H and 125 MHz for ^{13}C) spectrometer using *N*,*N′*-dimethylformamide (DMF)-d_7 as a solvent. Signals from the residual H in DMF-d_7 served as an internal standard for these spectra. ^{29}Si, ^{183}W and HETCOR spectra were recorded on a JEOL ECA400 (400 MHz for ^1H, 100 MHz for ^{13}C, 79.4 MHz for ^{29}Si and 16.6 MHz for ^{183}W) spectrometer using a mixed solvent of *N*,*N′*-dimethylpropyleneurea (DMPU, 1,3-dimethyl-3,4,5,6-tetrahydro-2(1*H*)-pyrimidinone), DMF-d_7, to which tetramethylsilane (TMS) was added as an internal standard (approximate volumetric ratio was DMPU:DMF:TMS = 60:35:5). TMS was used as an internal standard for the HETCOR and ^{29}Si spectra. For the ^{183}W NMR spectrum, 1.0 mol/L Na_2WO_4 in D_2O was used as an external standard by the sample replacement method.

Table S1. Type codes for Ag atoms and C≡C^{t}Bu ligands

Ag atoms		C≡C^{t}Bu ligands*	
Type code	Numbering	Type code	Numbering
A	1–6	a	1–3
B	7–18	b	4–9
C	19–24	c	10–21
D	25–30	d	22–27
E	31–42		

*Each C atoms in the C≡C^{t}Bu ligands is labeled as C*n*_*m*, where *n* designates the location of the C atom in the ligand (1 for the terminal *sp* C, 2 for the inner *sp* C, 3 for the tertiary sp^3 C, 4–6 for the methyl C) and *m* designates the sequential number for the ligand (*m* ranges from 1 to 27). This column shows the correspondence between the type codes (a–d) and the sequential number *m* (1–27).

Table S2. Site occupancies for type C Ag atoms

Atom	Occupancy	Atom	Occupancy
Ag19	0.902(6)	Ax19	0.098(6)
Ag20	0.908(5)	Ax20	0.092(5)
Ag21	0.529(6)	Ax21	0.471(6)
Ag22	0.863(5)	Ax22	0.137(5)
Ag23	0.935(6)	Ax23	0.065(6)
Ag24	0.841(5)	Ax24	0.159(5)
Sum(Ag19–Ag24)	4.978	Sum(Ax19–Ax24)	1.022

Table S3. Summary of interatomic distances in **1**

Atom	atom	distance range / Å	average distance / Å
Ag – Ag distances			
Ag	Ag		
type A	type A	3.134(2)-3.306(2)	3.212
	type B	2.971(3)-3.052(2)	3.022
	type C	2.860(4)-2.972(2)	2.918
type B	type B	3.006(3)-3.085(3)	3.041
	type D	2.914(3)-3.022(3)	2.968
	type E	2.849(3)-2.941(3)	2.898
type C	type C	2.550(6)-2.902(3)	2.770
	type E	2.917(3)-3.058(4)	2.983
	type X	1.76(4)-1.977(12)	1.827
type E	type X	2.41(4)-2.726(5)	2.601
C (terminal *sp* of C≡C^{t}Bu) – Ag distances			
C	Ag		
type a	type B	2.25(2)-2.37(2)	2.31
type b	type A	2.089(18)-2.141(15)	2.12
	type B	2.47(2)-2.70(2)	2.57
	type C	2.34(2)-2.52(3)	2.45
type c	type B	2.17(2)-2.24(2)	2.20
	type D	2.20(3)-2.33(3)	2.27
	type E	2.15(3)-2.24(3)	2.20
type d	type C	2.136(19)-2.20(2)	2.18
	type E	2.16(3)-2.29(3)	2.21
	type X	2.13(2)-2.19(3)	2.16
Ag – O distances			
Ag	O		
A	CO_3	2.183(15)-2.211(13)	2.20
	terminal(Nb)	2.476(13)-2.557(14)	2.52
B	terminal(Nb)	2.700(14)-2.871(13)	2.79
D	edge sharing(NbW)	2.674(15)-2.961(13)	2.83
	edge sharing(W_2)	2.989(15)-3.112(13)	3.07
	terminal(Nb)	3.410(13)-3.483(13)	3.44
E	edge sharing(NbW)	2.430(12)-2.490(12)	2.47
	terminal(W)	2.928(16)-3.162(15)	3.06
	corner sharing(W_2)	3.549(15)-3.650(14)	3.59
X	corner sharing(Nb_2)	2.14(3)-2.211(13)	2.17
	edge sharing(NbW)	2.72(3)-2.912(19)	2.82
	corner sharing(W_2)	3.01(6)-3.22(4)	3.13

Table S3. Summary of interatomic distances in **1** (continued)

Atom	atom	distance range / Å	average distance / Å
C – O distances in CO_3			
C1	O81 – O83	1.26(2)-1.27(2)	1.26
Si – O distances			
Si2	$\mu_4(SiNbW_2)$	1.583(14)-1.645(13)	1.62
	$\mu_4(SiW_3)$	1.622(13)-1.658(13)	1.64
Nb – O distances			
Nb	terminal(Nb)	1.775(12)-1.813(13)	1.79
	corner sharing(Nb_2)	1.908(13)-1.997(14)	1.94
	edge sharing(NbW)	2.008(12)-2.053(13)	2.03
	$\mu_4(SiNbW_2)$	2.410(13)-2.463(12)	2.43
W(belt) – O distances*			
W2	terminal(W)	1.677(13)-1.745(16)	1.71
W13	edge sharing(NbW)	1.865(13)-1.932(12)	1.91
W12	edge sharing(W_{belt},W_{belt})	1.847(18)-1.946(16)	1.92
W15	corner sharing(W_{belt},W_{belt})	1.861(15)-1.952(15)	1.91
W4	corner sharing(W_{belt},W_{cap})	1.906(15)-1.965(15)	1.93
W2	$\mu_4(SiNbW_2)$	2.333(11)-2.380(14)	2.36
W(cap) – O distances			
W8	terminal(W)	1.695(16)-1.725(13)	1.71
W18	corner sharing(W_{belt},W_{cap})	1.869(15)-1.934(15)	1.90
W16	edge sharing(W_{cap},W_{cap})	1.853(17)-1.948(15)	1.92
W7	$\mu_4(SiNbW_2)$	2.323(15)-2.373(14)	2.36

*W(belt) denote the W atoms that are adjacent to the Nb atoms (W1–W6 and W10–W15). W(cap) denote the W atoms that are on the opposite side of the $[SiW_9Nb_3O_{40}]^{7-}$ to the Nb atoms.

Table S4. Lattice dimensions of **1a**

	Single crystal diffraction at 123 K	Powder diffraction at room temperature
a / Å	21.172(1)	21.702(3)
b / Å	24.383(1)	25.165(3)
c / Å	31.630(1)	31.659(16)
α / °	90.138(1)	90.08(3)
β / °	95.802(2)	95.81(3)
γ / °	93.545(1)	91.773(13)
V / Å^3	16213.2(11)	17193(10)

Table S5. Comparison of ^{29}Si and ^{183}W NMR chemical shifts

condition	δ_{Si}	$\delta_{W\ (adjacent\ to\ Nb)}$	$\delta_{W\ (opposite\ to\ Nb)}$	$\Delta(\delta_W)$
Reaction mixture of $[(C_4H_9)_4N]_6H_2Si_2W_{18}Nb_6O_{77}$ + 8 $(C_4H_9)_4NOH$ (40 % in H_2O) in CD_3CN [a]	——	–112.0	–122.1	10.1
The product of the reaction of $[(C_4H_9)_4N]_6H_2Si_2W_{18}Nb_6O_{77}$ + 8 $(C_4H_9)_4NOH$ (40 % in H_2O) in CD_3CN that was stripped to dryness and re-dissolved in CD_3CN [a]	——	–97.9	–114.5	16.6
$Li_7SiW_9Nb_3O_{40}\cdot xH_2O$ [x = 11–12] in D_2O [b]	–82.9	–122.2	–128.2	6.0
$Na_7SiW_9Nb_3O_{40}\cdot xH_2O$ [x = 16–17] in D_2O [b]	–82.8	–121.6	–127.7	6.1
$K_7SiW_9Nb_3O_{40}\cdot xH_2O$ [x = 5–6] in D_2O [b]	–82.8	–118.0	–124.9	6.9
$Cs_7SiW_9Nb_3O_{40}\cdot xH_2O$ [x = 7–8] in D_2O [b]	——	–110.6	–118.3	7.7
$Li_7SiW_9Nb_3O_{40}\cdot xH_2O$ [x = 11–12] in DMSO-d_6 [b,d]	——	–95.0	–115.2	20.2
$Na_7SiW_9Nb_3O_{40}\cdot xH_2O$ [x = 16–17] in DMSO-d_6 [b,d]	–82.5	–93.9	–114.2	20.3
$K_7SiW_9Nb_3O_{40}\cdot xH_2O$ [x = 5–6] in DMSO-d_6 [b,d]	——	–95.1	–113.1	18.0
$[(C_4H_9)_4N][Ag_{42}(CO_3)(C\equiv C^tBu)_{27}(SiW_9Nb_3O_{40})_2]\cdot 5CH_3CN$ in DMPU/DMF-d_7 [c,e]	–81.3	–56.6	–102.6	46.0

[a] R. G. Finke and M. W. Droege, *J. Am. Chem. Soc.*, 1984, **106**, 7274-7277.

[b] K. Nomiya, K. Ohsawa, T. Taguchi, M. Kaneko and T. Takayama, *Bull. Chem. Soc. Jpn.*, 1998, **71**, 2603-2610.

[c] This work.

[d] DMSO = dimethyl sulfoxide

[e] DMPU = *N*,*N′*-dimethylpropyleneurea; DMF = *N*,*N*-dimethylformamide

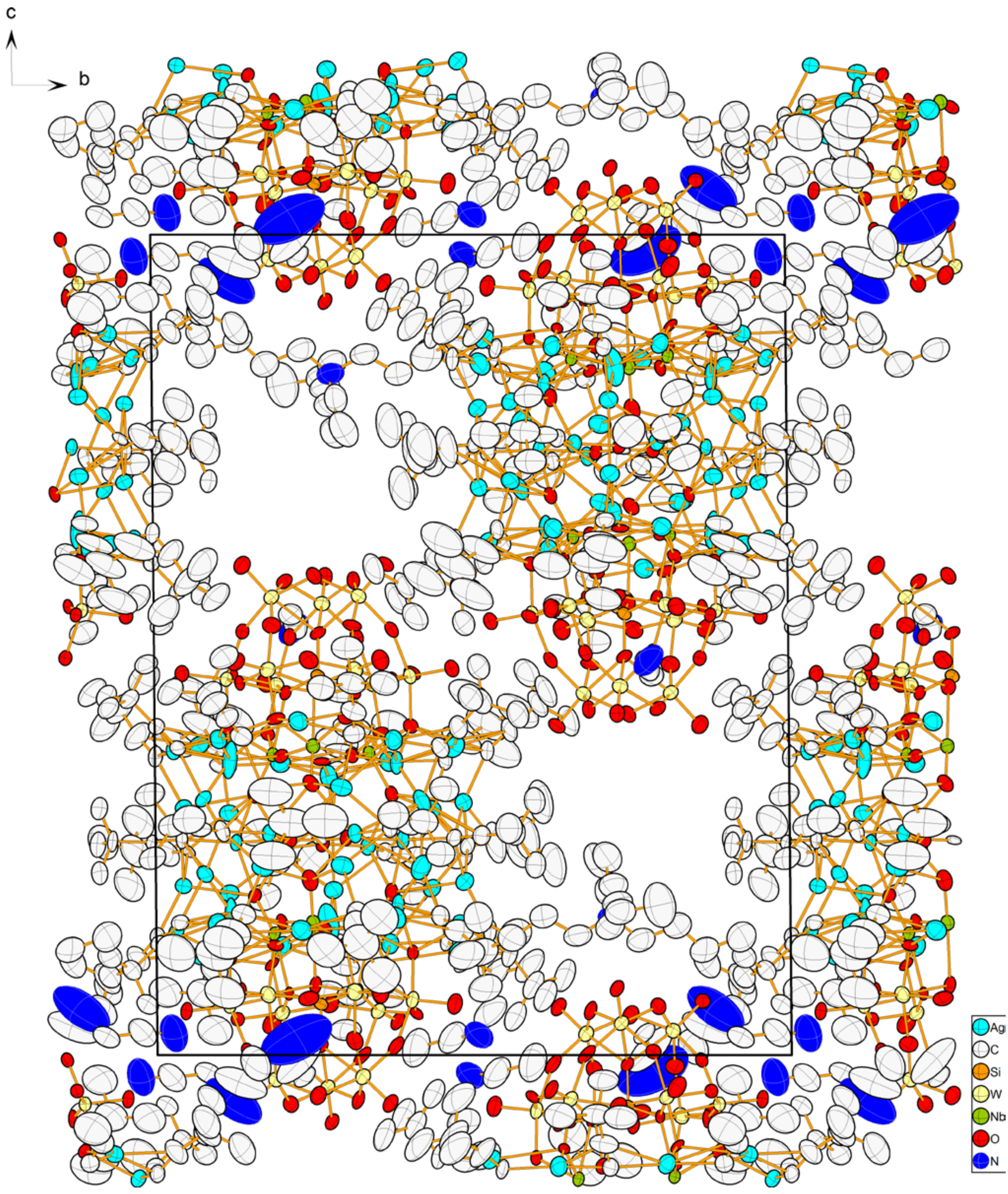

Figure S1. Packing diagram of **1a**. Ellipsoids are scaled to enclose 50 % probability levels.

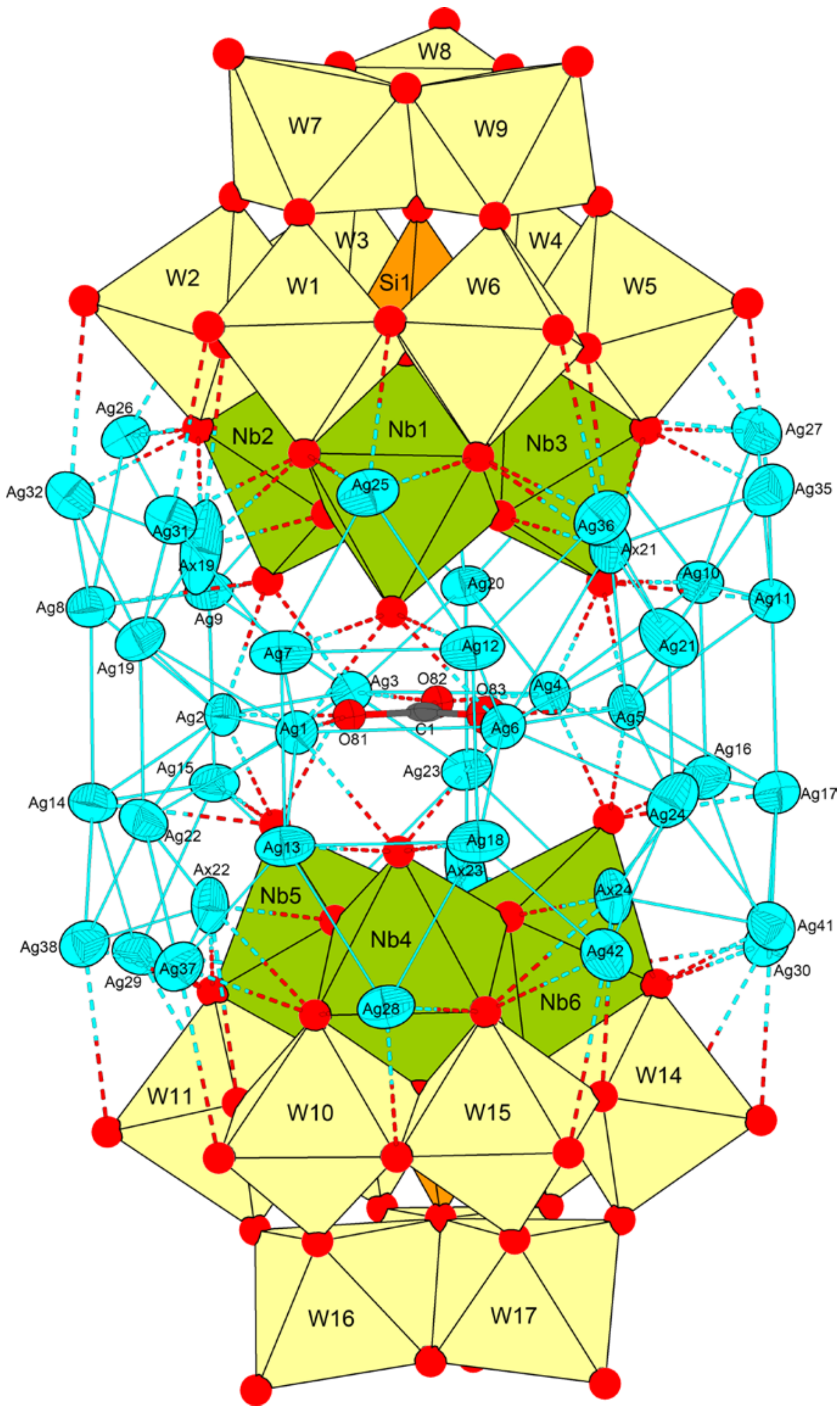

Figure S2. Displacement ellipsoid plot for the Ag atoms and the central CO_3^{2-} of **1**, together with the polyhedral representations of the two $[SiW_9Nb_3O_{40}]^{7-}$ polyoxometalate moieties. Ellipsoids are scaled to enclose 50 % probability levels. On each coordination polyhedron, the label of the atom at its center is displayed. Ag1–Ag6: type A; Ag7–Ag18: type B; Ag19–Ag24: type C; Ag25–Ag30: type D; Ag31–Ag42: type E.

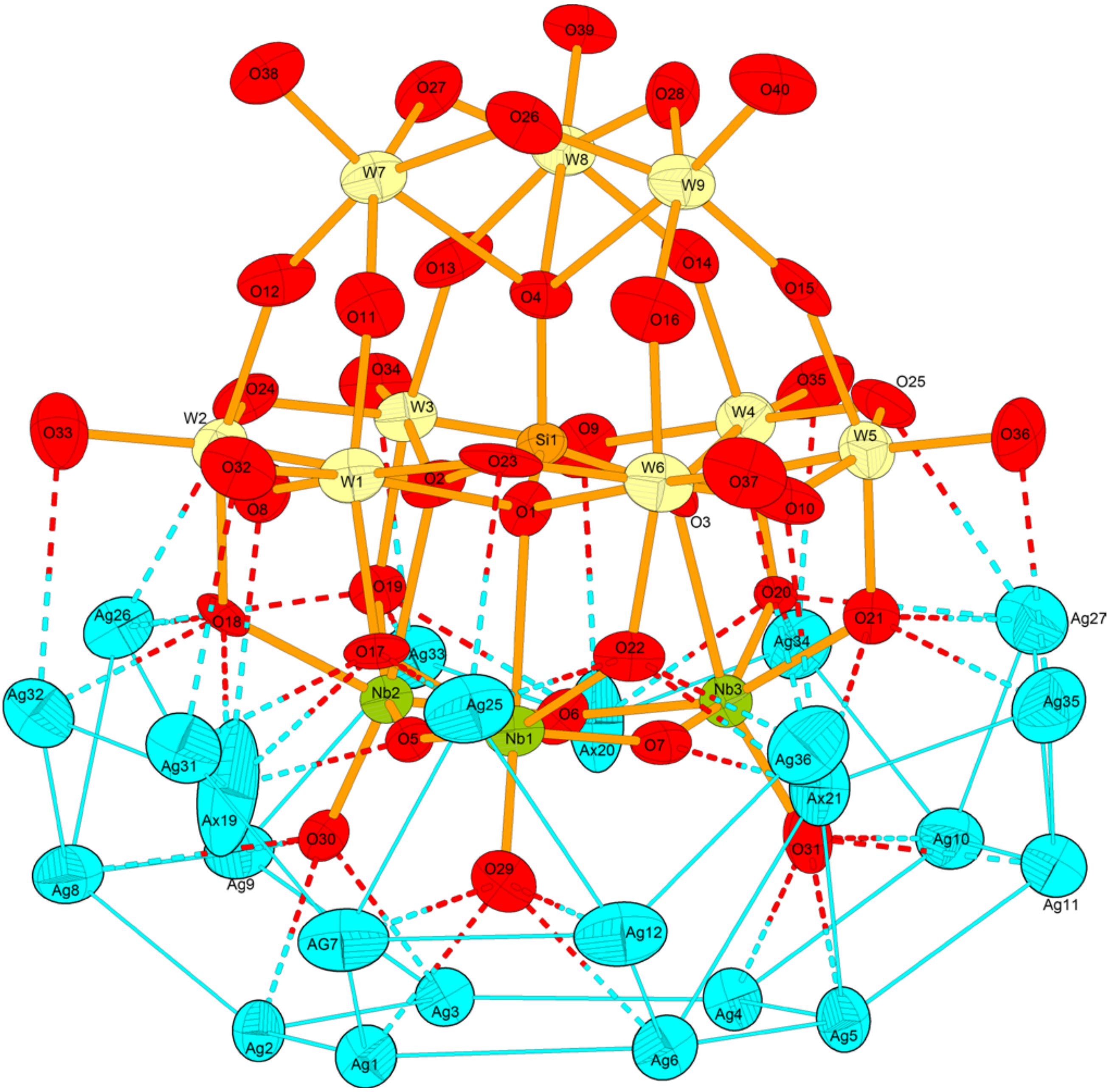

Figure S3. Displacement ellipsoid plot for one of the two $[SiW_9Nb_3O_{40}]^{7-}$ polyoxometalates in **1**, together with Ag atoms that are directly bonded to it. Viewing direction is the same as that of Figure S2. Ellipsoids are scaled to enclose 50 % probability levels.

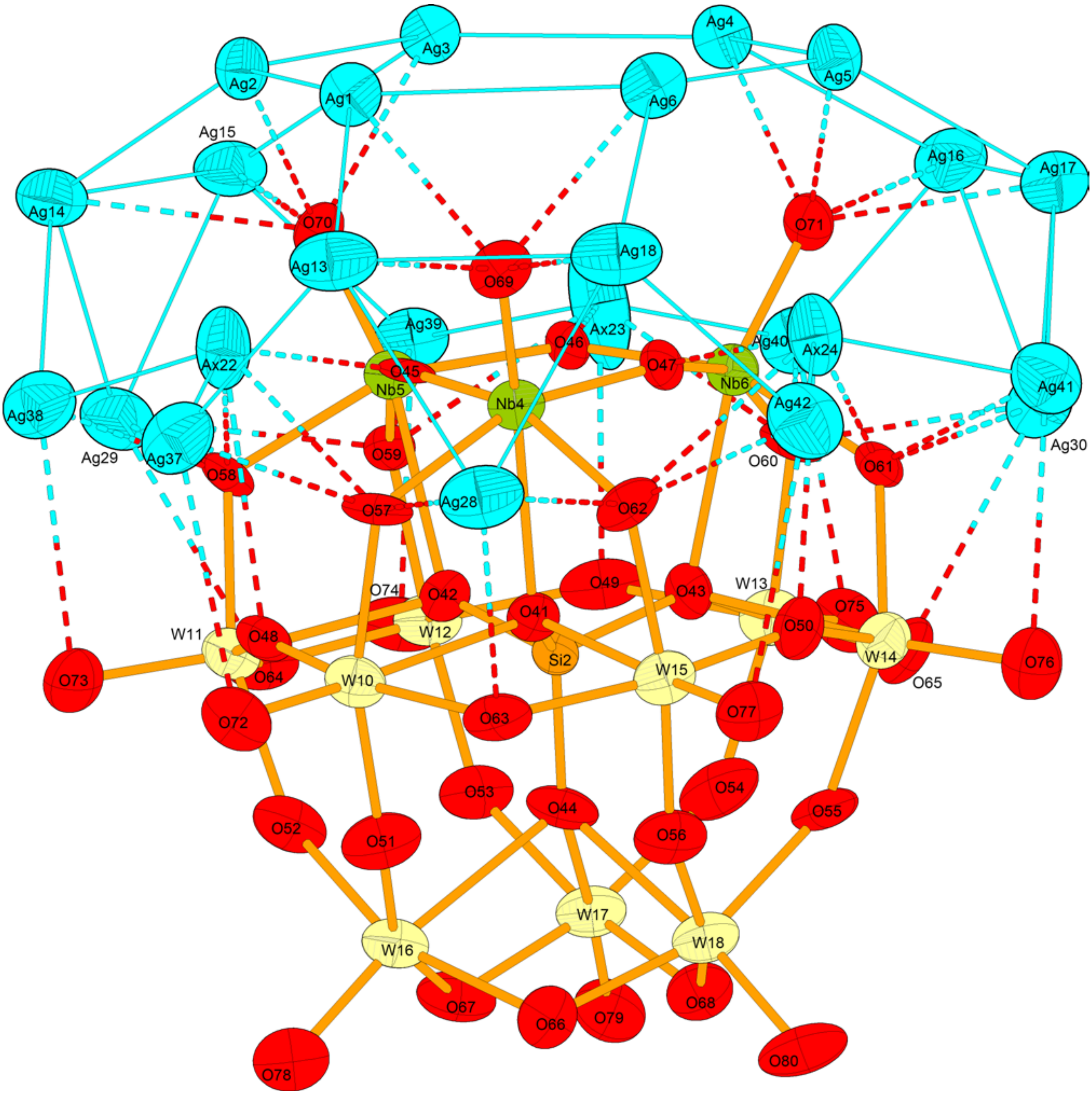

Figure S4. Displacement ellipsoid plot for the other $[SiW_9Nb_3O_{40}]^{7-}$ polyoxometalate in **1**, together with Ag atoms that are directly bonded to it. Viewing direction is the same as that of Figure S2 and S3. Ellipsoids are scaled to enclose 50 % probability levels.

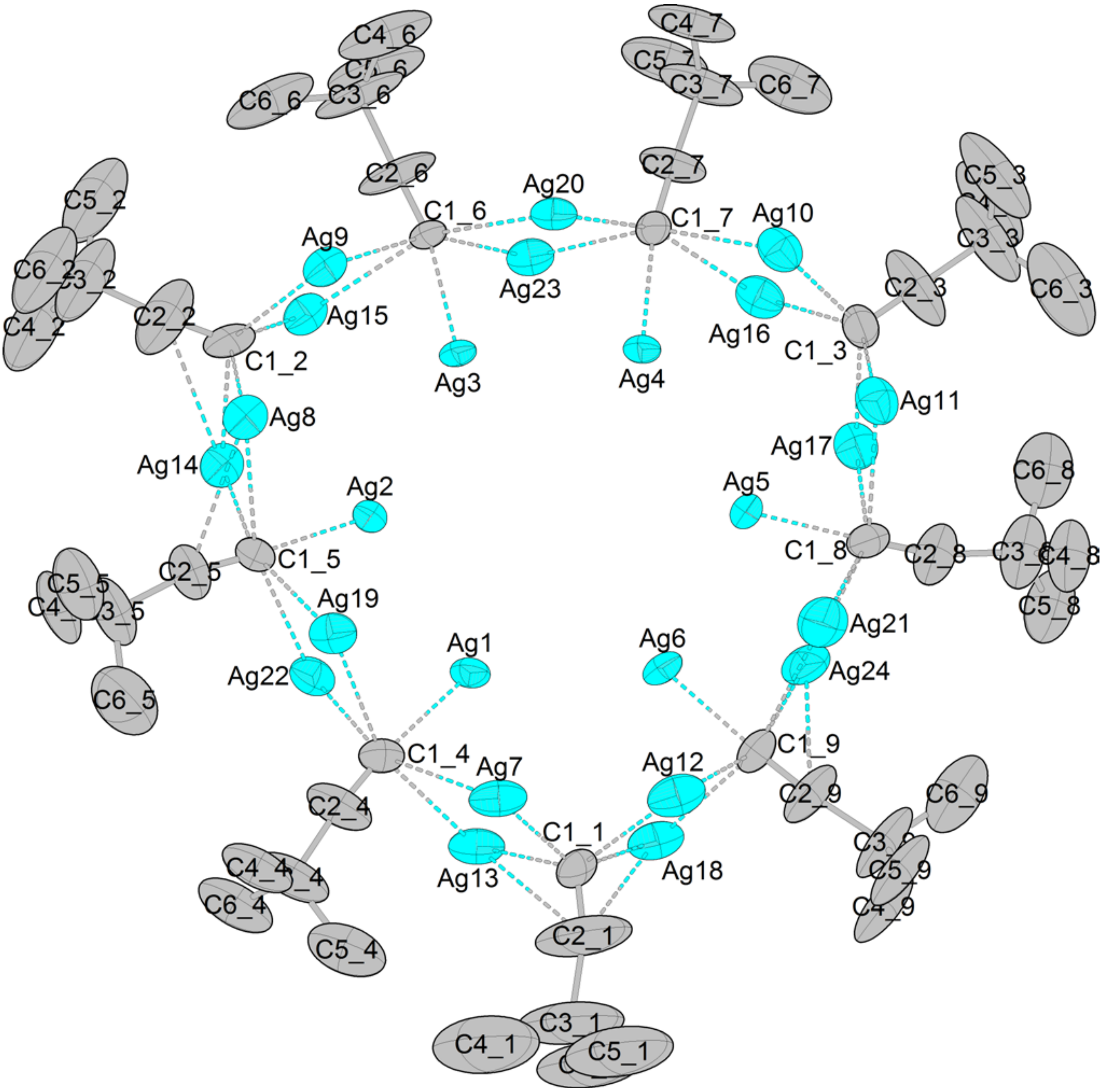

Figure S5. Displacement ellipsoid plot for the nine C≡C^{t}Bu ligands on the central layer in **1**, together with Ag atoms that are directly bonded to them. Ellipsoids are scaled to enclose 50 % probability levels.

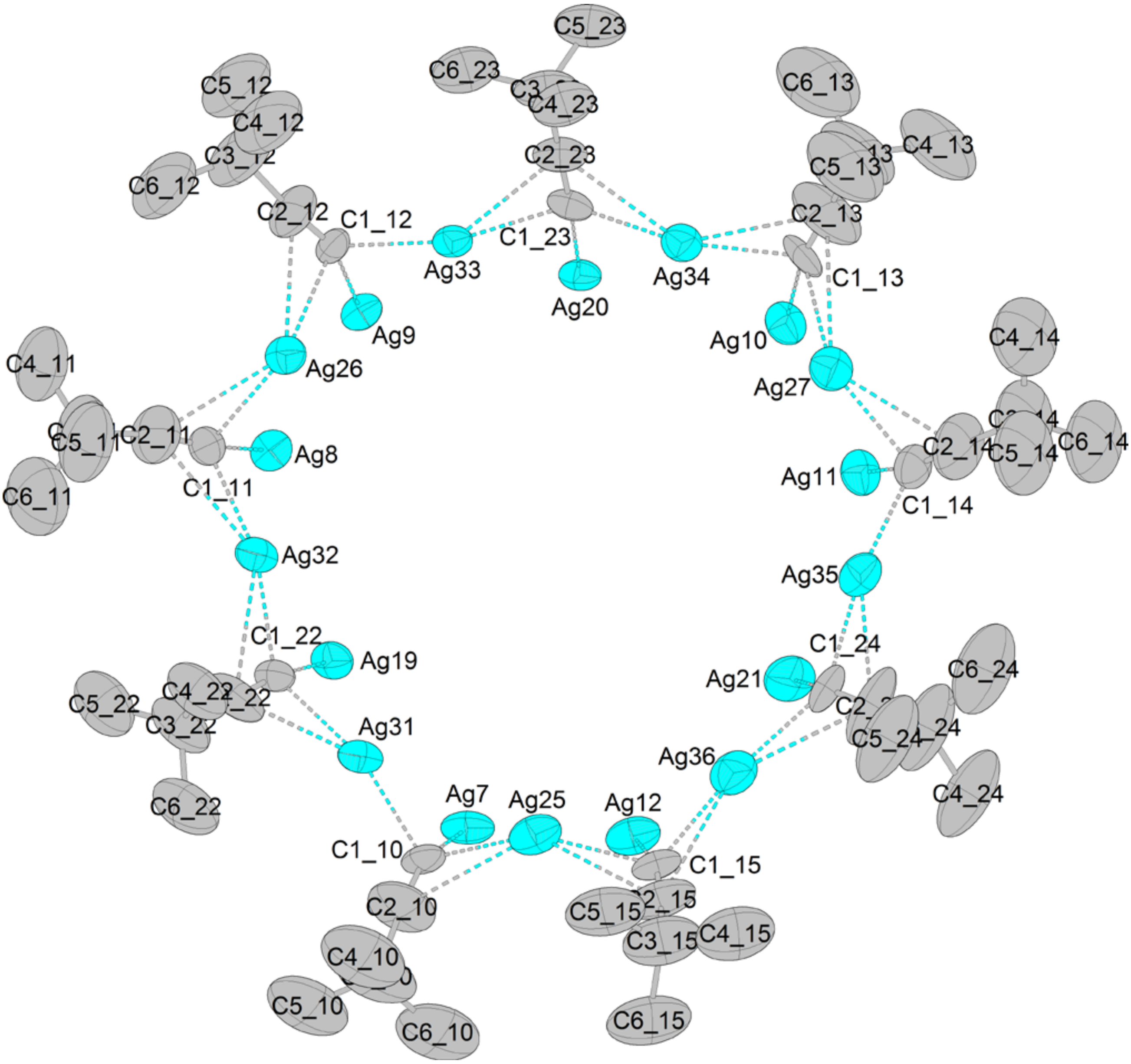

Figure S6. Displacement ellipsoid plot for the nine C≡C^{t}Bu ligands on one of the two peripheral layers in **1**, together with Ag atoms that are directly bonded to it. Ellipsoids are scaled to enclose 50 % probability levels.

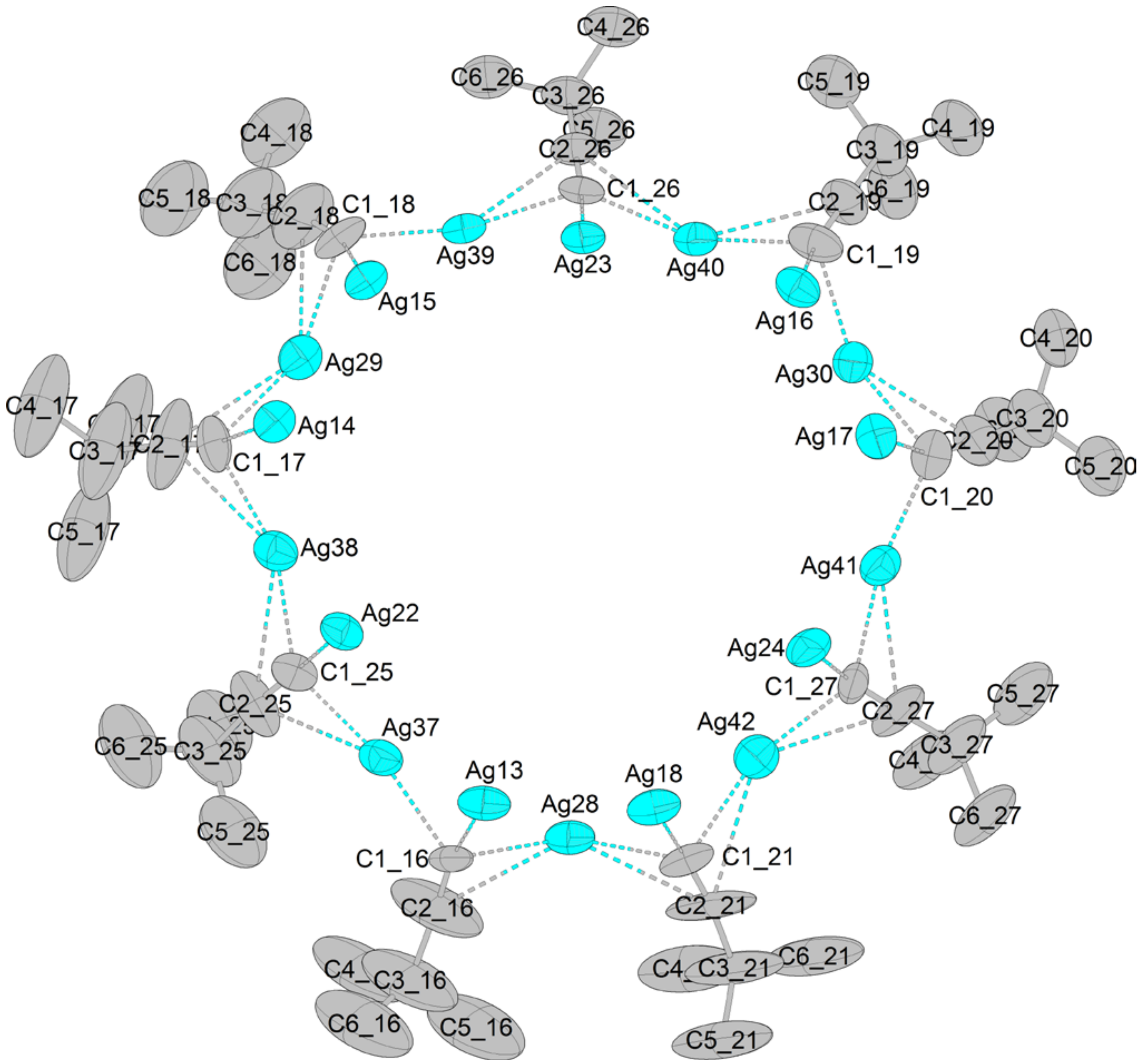

Figure S7. Displacement ellipsoid plot for the nine C≡C^{t}Bu ligands on the other peripheral layer in **1**, together with Ag atoms that are directly bonded to it. Ellipsoids are scaled to enclose 50 % probability levels.

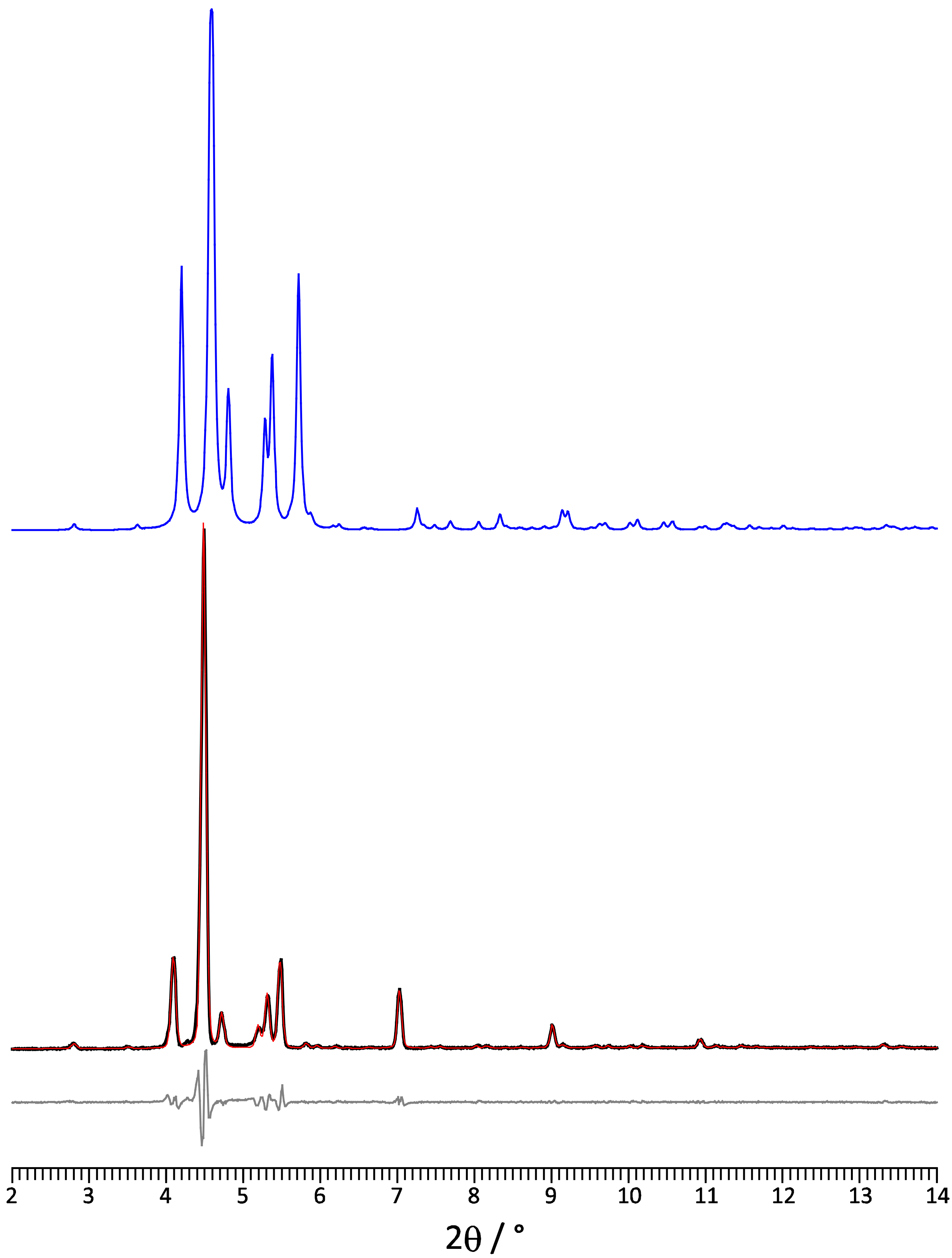

Figure S8. Comparison of observed and calculated powder diffraction patterns of **1a**. Top blue trace: simulated pattern based on CIF from single crystal diffraction at 123 K; middle black trace: observed pattern at room temperature; middle red thin trace: calculated pattern based on the Pawley fitting against the observed data; bottom gray trace: difference between the observed and fitted patterns.

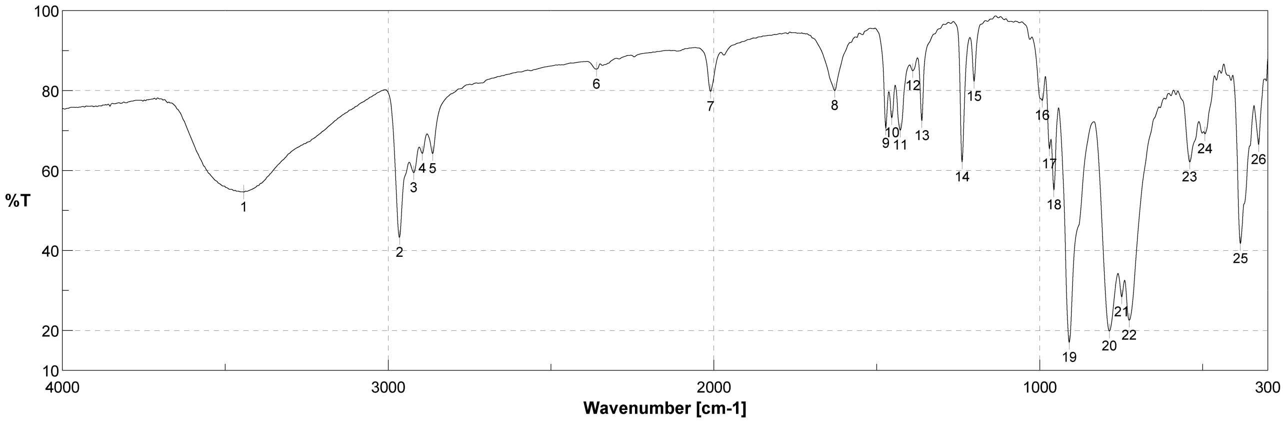

No.	cm-1	%T	No.	cm-1	%T	No.	cm-1	%T	No.	cm-1	%T	No.	cm-1	%T
1	3443.28	54.6132	2	2965.02	43.284	3	2921.63	59.4634	4	2895.59	64.2962	5	2863.77	64.2562
6	2360.44	85.3826	7	2010.43	79.7787	8	1629.55	80.013	9	1472.38	70.5659	10	1454.06	73.2306
11	1428.03	70.0879	12	1389.46	84.9912	13	1361.5	72.4852	14	1238.08	62.1626	15	1201.43	82.3243
16	992.196	77.5287	17	970.019	65.4264	18	956.52	55.1672	19	909.272	17.0085	20	785.85	19.8486
21	748.245	28.3972	22	725.104	22.5514	23	539.971	62.1539	24	492.723	69.1852	25	383.765	41.7421
26	327.839	66.4984												

Figure S9. Infrared absorption (IR) spectrum of **1a** measured as a KBr pellet

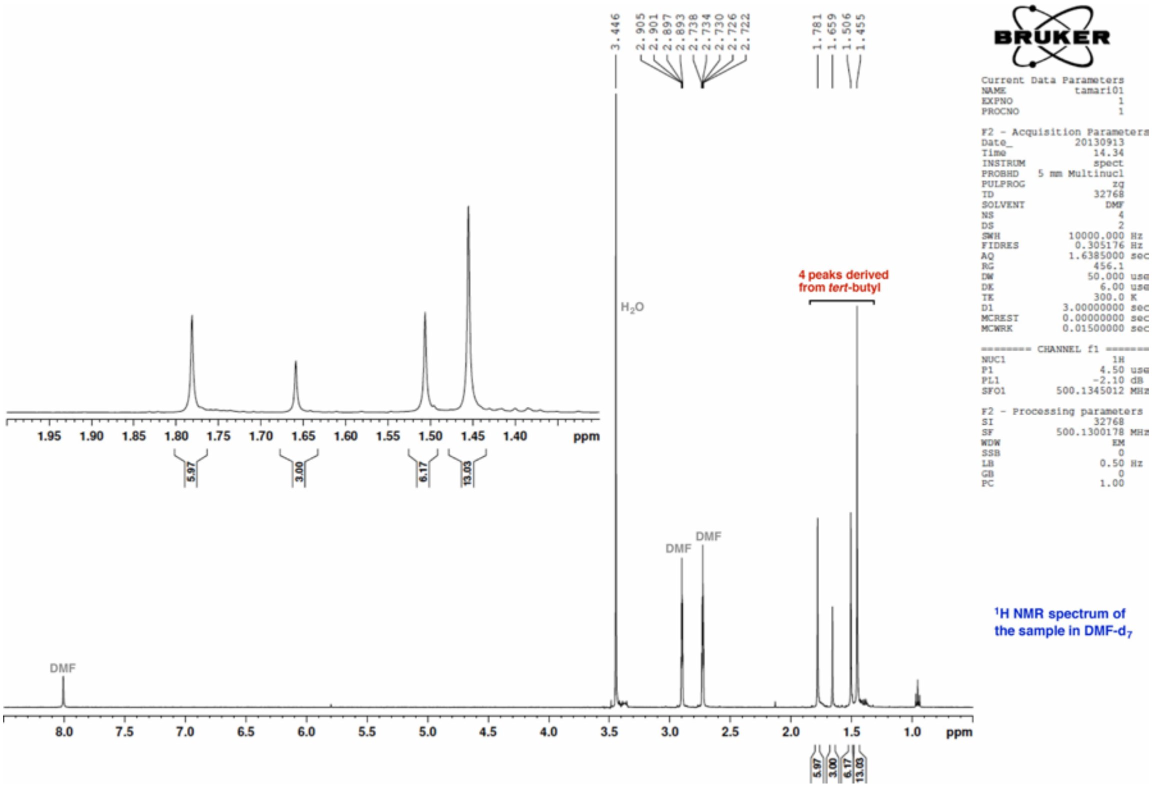

Figure S10. ^{1}H NMR spectrum of **1a** in DMF-d_7

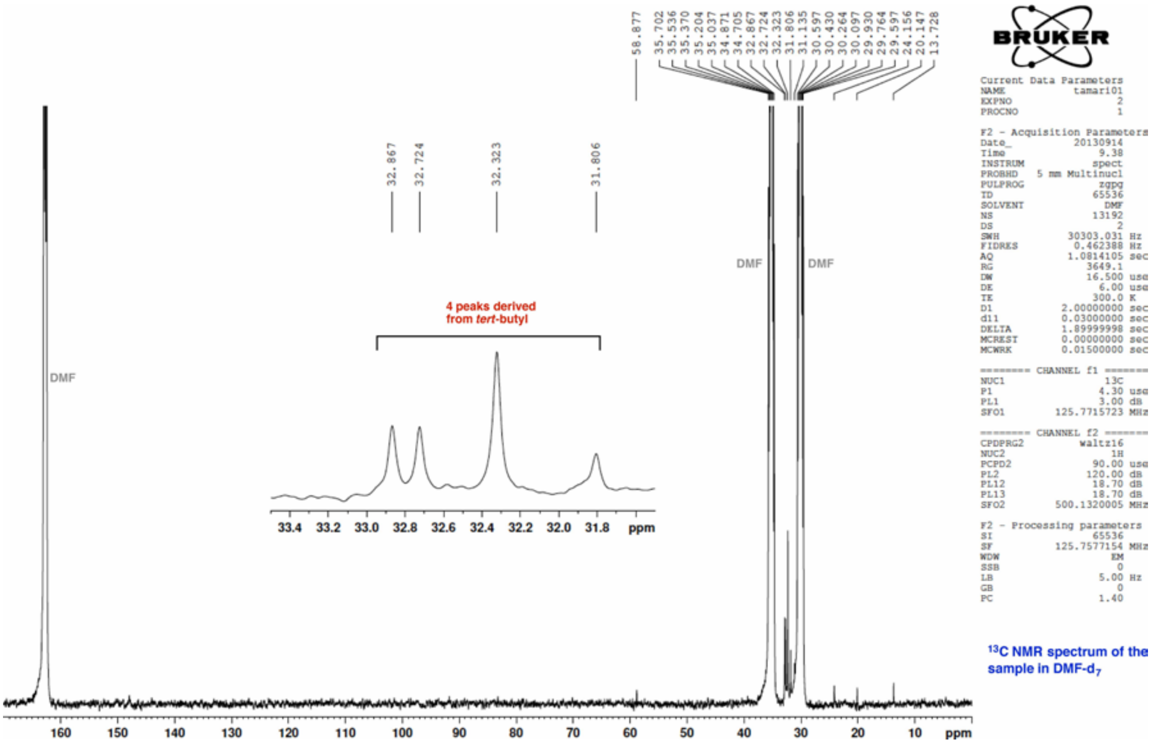

Figure S11. ^{13}C NMR spectrum of **1a** in DMF-d_7

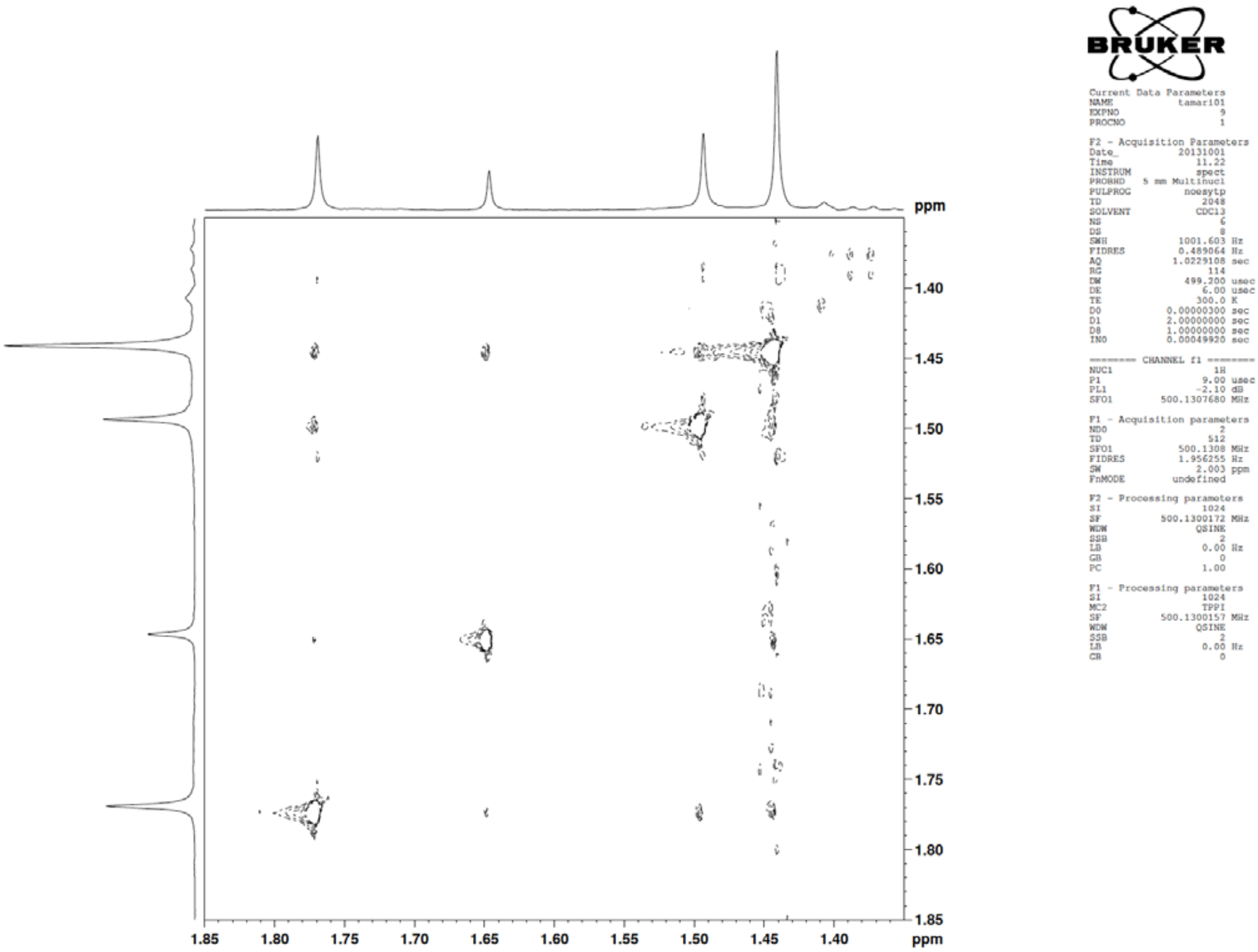

Figure S12. NOESY spectrum of **1a** in DMF-d_7

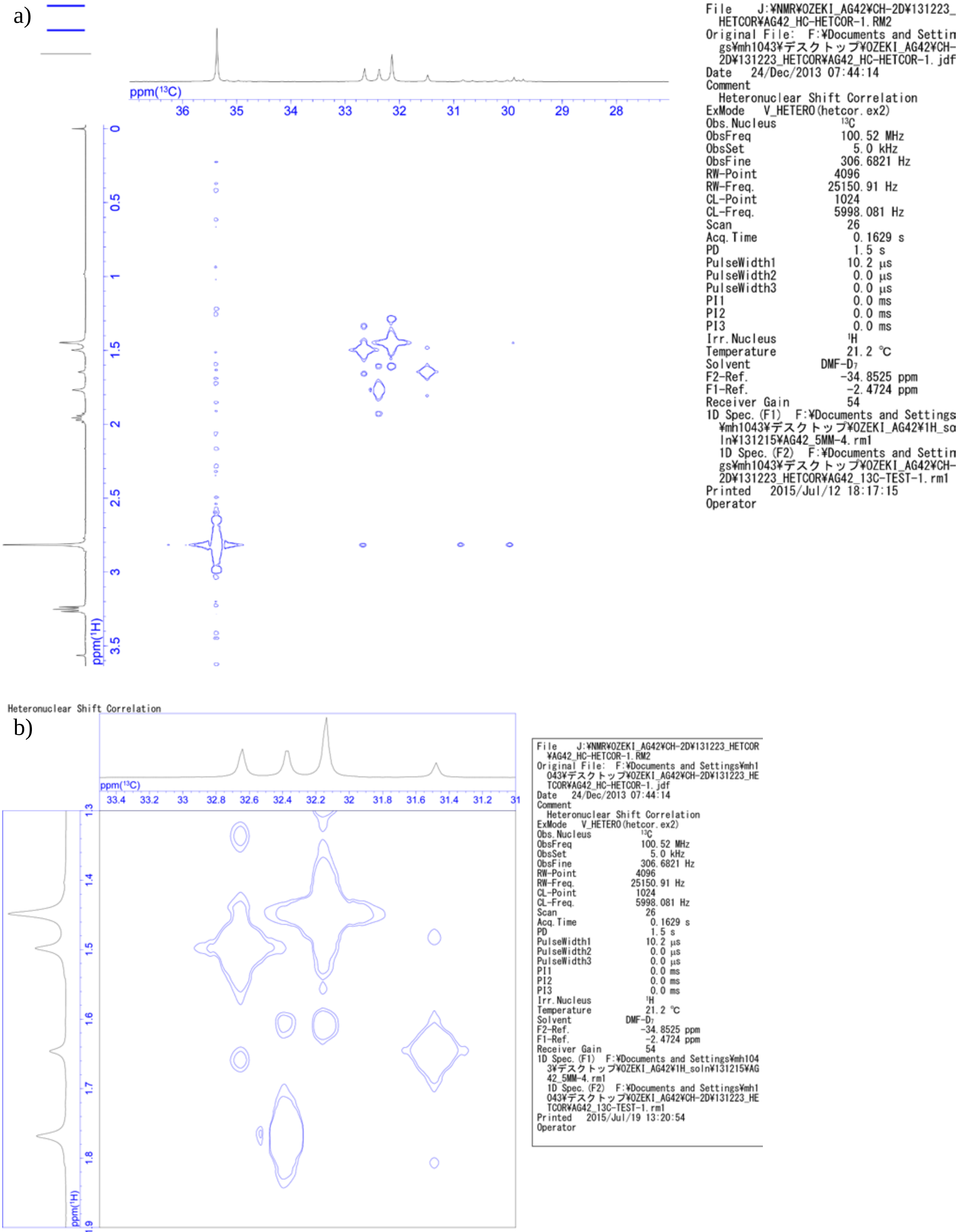

Figure S13. HETCOR spectrum of **1a** in DMPU/DMF-d_7 showing a) 3.5–0 ppm for ^{1}H and 37–27 ppm for ^{13}C and b) 1.9–1.3 ppm for ^{1}H and 33.5–31.0 ppm for ^{13}C. Peaks at 35.4 ppm in ^{13}C and 2.8 and 3.2 ppm in ^{1}H are due to DMPU.

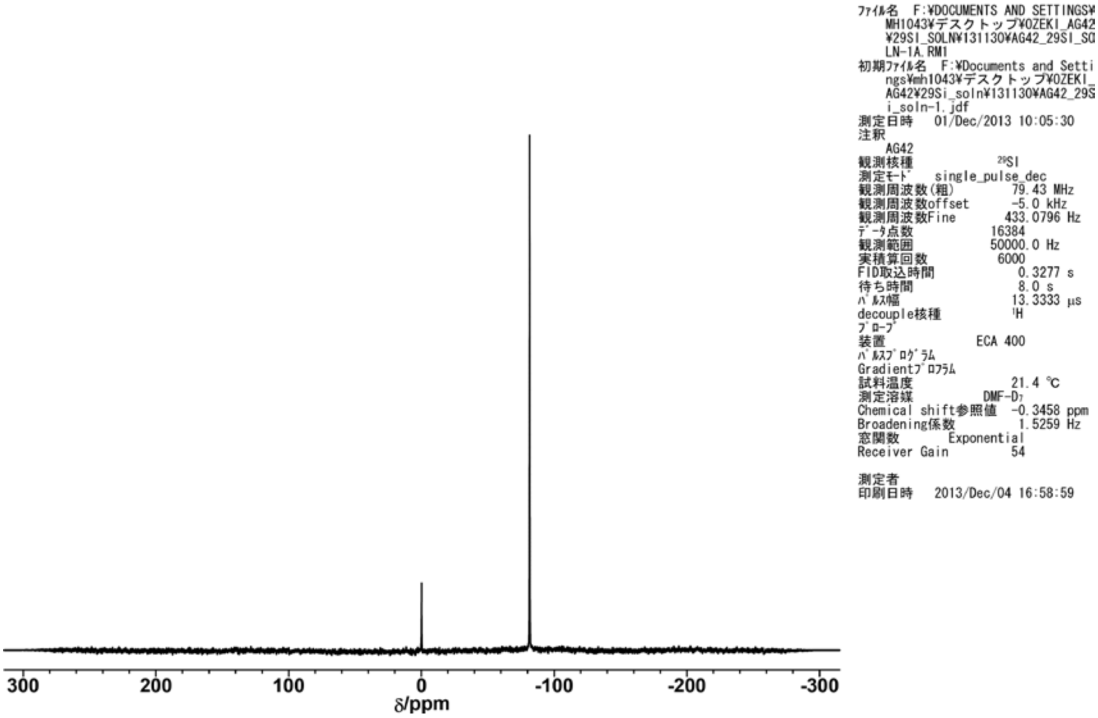

Figure S14. ^{29}Si NMR spectrum of **1a** in DMPU/DMF-d_7. The signal at 0 ppm is due to TMS, the internal standard.

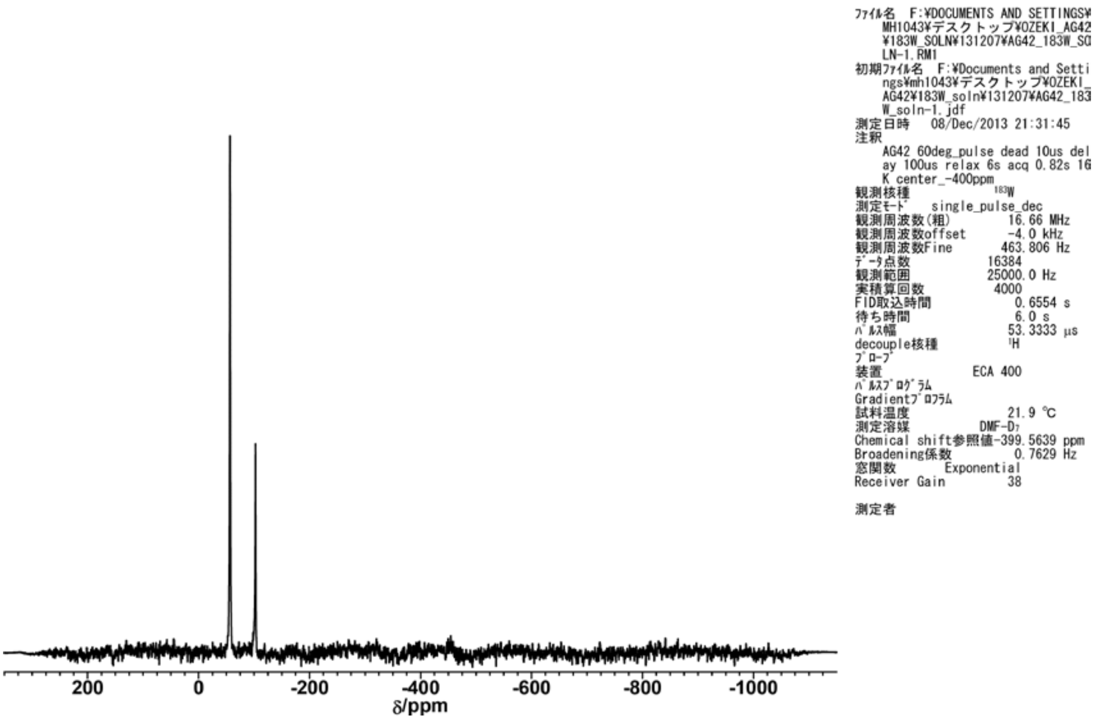

Figure S15. ^{183}W NMR spectrum of **1a** in DMPU/DMF-d_7

References

1. Molecular Structure Corporation, *CrystalClear*, (2001), Orem, UT.
2. Z. Otwinowski and W. Minor, *Methods Enzymol.*, 1997, **276A**, 307-326.
3. A. L. Spek, *PLATON, A Multipurpose Crystallographic Tool*, (2013) Utrecht University, Utrecht, The Netherlands.
4. L. Palatinus and G. Chapuis, *J. Appl. Crystallogr.*, 2007, **40**, 786-790.
5. G. M. Sheldrick, *Acta Crystallographica Section C*, 2015, **71**, 3-8.
6. L. Farrugia, *J. Appl. Crystallogr.*, 2012, **45**, 849-854.
7. C. F. Macrae, I. J. Bruno, J. A. Chisholm, P. R. Edgington, P. McCabe, E. Pidcock, L. Rodriguez-Monge, R. Taylor, J. van de Streek and P. A. Wood, *J. Appl. Crystallogr.*, 2008, **41**, 466-470.
8. K. Brandenburg, *DIAMOND 3.2k*, (2014) Crystal Impact GbR, Postfach 1251, 53002 Bonn, Germany.
9. Bruker AXS, *TOPAS V5: General profile and structure analysis software for powder diffraction data*, (2014), Karlsruhe, Germany.